

Point by point narrative of edits in response to reviewers' major comments:

A list of tables and website addresses for data and code plus Fig S1 (Fig 9 in original submission) have been added as a supplementary page.

Line numbers refer to the markup version of the manuscript.

Zeeden:

The title of the manuscript has been changed to reflect the 0 to 5 Ma ages considered.

2 new tables have been added:

Leg154_Combined_Benthic_Isotopes

Leg154_Smoothed_Benthic_Isotopes

The MS data are already included in individual site tables. Each data set has the equivalent Site 926 depths included.

Line 110 added web location of data files and software

Line 149 added references on lighting correction by earlier authors.

Line 162 added several sentences addressing the possibility of 9/10 m long lighting variation signals.

Lines 236 & 242 added to cover the relationship between MS and insolation and add a reference to the approach of Zeeden et al.

Line 265 Moved fig 9 to supplement.

Line 286 added paragraph addressing uncertainty.

Bickert:

Line 142 answered question regarding distortion of core along outer edges

Line 182 added reference to Ruddiman. We did not want to add more detail within the manuscript itself beyond what we already have since splicing is understood by most of the community and those not familiar may check the reference.

Figures 8 and 10 have been changed to add more data and are now figures 8 and 9.

Formatted: Indent: First line: 0 cm

All of the minor suggestions have been addressed as well.

Revisiting the Ceara Rise, equatorial Atlantic Ocean: isotope stratigraphy of ODP Leg 154 from 0 to 5 Ma

R. H. Wilkens¹, T. Westerhold², A. J. Drury², M. Lyle³, T. Gorgas⁴, and J. Tian⁵

¹Hawaii Institute of Geophysics & Planetology, University of Hawaii, Honolulu, HI, 96822, U.S.A.

²MARUM, University of Bremen, Bremen, 28359, Germany

³CEOAS, Oregon State University, Corvallis, OR, 97331, U.S.A.

⁴~~GFZ German Research Centre for Geosciences, 14473 Potsdam, Germany~~~~Helmholtz Centre Potsdam, GFZ, Potsdam, 14473, Germany~~

⁵State Key Laboratory of Marine Geology, Tongji University, Shanghai, 200092, China

Correspondence to: Roy H. Wilkens (rwilkens@hawaii.edu)

Abstract

Isotope stratigraphy has become the method of choice for investigating both past ocean temperatures and global ice volume. Lisiecki and Raymo (2005) published a stacked record of 57 globally distributed benthic $\delta^{18}\text{O}$ records versus age (LR04 stack). In this study LR04 is compared to high resolution records collected at all of the sites drilled during ODP Leg 154 on the Ceara Rise, in the western equatorial Atlantic Ocean. Newly developed software is used to check data splices of the Ceara Rise sites and better align out-of-splice data with in-splice data. Core images recovered from core table photos are depth and age scaled and greatly assist in the data analysis. The entire splices of ODP Sites 925, 926, 927, 928 and 929 were reviewed. Most changes were minor although several were large enough to affect age models based on orbital tuning. A Ceara Rise composite record of benthic $\delta^{18}\text{O}$ is out of sync with LR04 between 1.80 and 1.90 Ma, where LR04 exhibits 2 maxima but ~~where~~ Ceara Rise data contains only 1. The interval between 4.0 and 4.5 Ma in the Ceara Rise compilation is decidedly different from LR04, reflecting both the low amplitude of the signal over this interval and the limited amount of data available for the LR04 stack. A regional difference in benthic $\delta^{18}\text{O}$ of 0.2 ‰ relative to LR04 was found. Independent tuning of Site 926 images and physical property data to the Laskar et al. 2004 orbital solution and integration of available benthic stable isotope data from the Ceara Rise provides a new regional reference section for the equatorial Atlantic covering the last 5 million years.

27
28
29
30
31
32
33
34
35
36
37
38
39
40
41
42
43
44
45
46
47
48
49
50
51
52
53
54
55
56
57
58
59
60
61
62

1. Introduction

Sedimentary archives retrieved by ocean drilling since 1968 by the Deep Sea Drilling Program (DSDP, 1968-1983), the Ocean Drilling Program (ODP, 1983-2003), the Integrated Ocean Drilling Program (IODP, 2003-2013) and the International Ocean Discovery Program (IODP, since 2013) provide key records needed to better understand processes and interactions of the Earth system. Over almost 5 decades of coring, ocean drilling samples and data have contributed significantly to major breakthroughs in our understanding of earth history - including such basic tenets as seafloor spreading, a detailed history of reversals of the Earth's magnetic field, evolution/extinction of marine species and many more. Included in this list is the advancement of stable isotope stratigraphy and the recognition of the critical part played by variations in the Earth's orbital parameters in climate history. Sites drilled during ODP Leg 154 on the Ceara Rise have played a significant role in creating age models for the Neogene based on astrochronology.

Stable isotope stratigraphy has become the method of choice for investigating both past ocean temperatures and global ice volume. When global ice volumes are large, such as times of vast continental ice sheets, the world oceans become enriched in ^{18}O , a "heavy" isotope of the more abundant ^{16}O . It has been demonstrated (e.g. Hays et al, 1976) that variations in ^{18}O enrichment ($\delta^{18}\text{O}$) coincide with periodicities of the orbital parameters of eccentricity, obliquity, and precession and their influence on the distribution and intensity of solar insolation on the Earth's surface. Therefore, with a knowledge of the previous behavior of the orbital parameters (e.g. Laskar et al., 2011) isotope stages (cycles) may be assigned ages to a very high degree of precision (astronomical tuning). Lisiecki and Raymo (2005) published a compilation of globally distributed benthic $\delta^{18}\text{O}$ records versus age from 57 sites worldwide that included data from the past 5.3 Ma (LR04 stack). Their work established a framework against which almost all subsequent isotopic studies of late Neogene sediments have been compared.

The LR04 stack is a significant contribution for having demonstrated the global semi-synchronicity of the overall behavior of the $\delta^{18}\text{O}$ record in deep sea benthic stable isotope data. It does, however, have some drawbacks. LR04 is an amalgam of data with various resolutions from sites in different oceans and different latitudes, thus averaging regional signals into the overall stack. The age models used for the individual data sets depend on chronological markers such as the ages of magnetic field reversals that may have shifted/changed since the original studies were completed and new data has been reported. Astronomical tuning is complicated by the dominance of obliquity in records from sediments older than 1.2 Ma because the pattern of consecutive cycles are similar. And finally, almost all of the $\delta^{18}\text{O}$ profiles were derived from spliced data. Splicing is a technique used at ~~ocean~~-drilling sites to piece together one continuous record from adjacent drill holes (Ruddiman et al. 1987; Hagelberg et al., 1992). Splices may be subject to cycle skipping or duplication of events when data are aligned from different holes. Averaging of multiple sites will compensate for small errors in the spliced records if many sites are used and most have a correct splice. As with age models, splices may evolve over time as more detailed and new types of data are gathered post-cruise and reveal previously missed or doubled $\delta^{18}\text{O}$ patterns (see Westerhold et al. 2014, supplementary ~~fig~~Figure S9).

63 | There are 21 records [included in LR04](#) that extend to ages older than 3 Ma included in LR04, and only 14
64 | that have data older than 4 Ma. As the numbers in the stack shrink, the importance of having well-spliced records
65 | grows. A number of records used in LR04 contain problematic succession with respect to their composite record.
66 | Site 982, for example, is one of the high-resolution sites that extends beyond 3 Ma (Venz et al. 1999, Venz and
67 | Hodell 2002), and has been used subsequently to transfer age models to other isotope records (Drury et al. 2016).
68 | However, there is controversy over the composite record of 982 as well as the age model (Lawrence et al. 2013,
69 | Khelifi et al. 2012, Bickert et al. 2004).

70 | For the interval 1.7-5.3 Ma the LR04 stack depends heavily on the spliced records from Leg 138 - the S95
71 | benthic composite stack (Shackleton et al., 1995). It was noted in Lisiecki and Raymo (2005) that for marine isotope
72 | stages (MIS) M2 and MG2 at 3.35 Ma there is a mismatch of data and a potential coring or splicing problem in Site
73 | 846. Even so, Site 846 was used for the initial alignment in LR04 from 2.7-5.3 Ma along with Site 849 (1.7 - 3.6
74 | Ma) and Site 999 (3.3 - 5.3 Ma). Any problem in the spliced records of the sites used for initial alignment will
75 | propagate through the stack if not compensated by a large number of additional sites. Thus we might expect a
76 | greater possibility of erroneous correlation in older less repeated parts of the stack, particularly where the amplitude
77 | of the $\delta^{18}\text{O}$ variations are relatively small (see Lisiecki and Raymo 2005 [Fig. 2](#)).

78 | In order to provide a precise age model the LR04 stack was tuned to a non linear ice volume model forced
79 | by insolation (65°N) using the Laskar et al. (1993) 1,1 orbital solution including an assumed decrease in the lag of
80 | ice sheet response to insolation forcing. To test and evaluate the LR04 stack and the tuning approach from 0 - 5 Ma,
81 | a robust composite record from a single location combined with an astronomical age model that is independent of
82 | ice volume modeling is required. Furthermore, extending the $\delta^{18}\text{O}$ stack into the Miocene means that robust
83 | composite records are required to avoid misalignments and tuning errors at the outset. Sediments from the Ceara
84 | Rise (South Atlantic) are perfectly suited for testing because they contain orbitally driven changes and are already
85 | the backbone for astronomical calibration of the Geological Time Scale for the last 14 Ma (Shackleton and
86 | Crowhurst 1997, Zeeden et al. 2013, [2014](#), Lourens et al. 2004).

87 | Here we revisit data collected during, and subsequent to, ODP Leg 154 ([Fig. 1](#)). The LR04 stack
88 | includes benthic stable isotope data from ODP Leg 154 Sites 925, 927, 928, and 929. Site 927 was used for initial
89 | alignment from 0–1.4 Ma in LR04. Site 926 is also considered a primary site for time scale constructions for 0-15
90 | Ma and is independent of LR04. In this study, we use newly developed software to check and improve the
91 | composite records of Leg 154, [We then](#) stretch and squeeze data outside the splice, use core images to correlate all
92 | sites to the Site 926 depth scale, orbitally tune the core images, and compare the age model with the LR04 stack for
93 | the past 5 Ma. The new software system greatly facilitates the construction of benthic $\delta^{18}\text{O}$ reference records back
94 | into the Miocene from single regions. [Regional a](#)Astronomically tuned ~~regional~~ $\delta^{18}\text{O}$ records are a next important
95 | step in deciphering paleoceanographic conditions worldwide.

96 |
97 | **2. Material and Methods**

98 | The proliferation and diversity of the data collected both during and after ocean drilling cruises can at times
99 | be somewhat overwhelming for the individual scientist. Data are now freely available through online data bases

100 maintained by the ocean drilling infrastructure for cruise results (e.g. [LIMS](#), [JANUS](#)), by national efforts (e.g.
101 [NGDC](#)) or community efforts (e.g. [PANGAEA](#)). However, a unified and consistent system for integrating disparate
102 data streams such as micropaleontology, physical properties, core images, geochemistry, and borehole logging has
103 not been widely available. In this section we describe a system that we have developed over several years to work
104 with ocean drilling data and images (CODD - Code for Ocean Drilling Data). CODD takes advantage of the
105 versatile graphical user interface and analytical functions contained in the [IGOR™](#) graphing and analysis program
106 commercially available from Wavemetrics, Inc. One of the great advantages of a modern analysis program like
107 IGOR™ paired with new computers and fast processors is the ability to use images as data. Rather than a static
108 picture of a core or section, images are scaled and plotted along with traditional data versus depth or age. Core
109 images may be squeezed, stretched, subsampled, and concatenated, allowing for great versatility. The CODD set of
110 ocean drilling macros for IGOR™ and a User Guide are freely available ~~at www.CODD-Home.net through the~~
111 ~~[PANGAEA website at XXX \(DOI to be inserted here\)](#)~~. ~~Core images, both as png files and scaled IGOR binaries as~~
112 ~~[well as all tables of this study including age models, offsets, splices, tie points between sites, spliced MS data,](#)~~
113 ~~[isotope data, and mapping pairs for squeezing and stretching of cores are available open access through the open](#)~~
114 ~~[access Pangaea website under <https://doi.pangaea.de/10.1594/PANGAEA.870873>.](#)~~

115

116 **2.1 Data Structure**

117 The heart of the CODD data structure is the coring matrix - a 3 layered array in which the top layer
118 contains the original depth to the top of each section (~~mbsf or esf - meters below seafloor~~) sorted by core (rows) and
119 sections (columns). The middle layer contains the length of the sections and the third layer the composite depth
120 (~~mcd or eesf - meters composite depth~~). Sample depths are calculated by referencing the proper layer and coordinate
121 by core and section and then adding the sample interval. The reverse process of returning the core, section, and
122 interval designation of a given sample depth is accommodated by comparing it to the section top depth plus the
123 section length to find where the sample originated.

124 A standardized naming convention is essential to efficient processing of multiple and diverse data streams.
125 In CODD data are assigned 3 part names, Hole, Technique and Information, separated by underscores. Thus
126 gamma-ray attenuation depths are U925A_GRA_MBSF and U925A_GRA_MCD with data as U925A_GRA_GRA.
127 Core, section, interval and age are similarly named. Isotope data might be U925A_Iso_d18O and U925A_Iso_d13C.
128 While the Hole and Technique designations must be identical for a single data set, the Information may be anything
129 the user desires, including new data like ratios created from existing information. IGOR™ records data processing
130 steps and the use of a standard naming convention allows users to repeat processing for different data by simply
131 replacing one Hole or Technique with another in the recorded steps. It also simplifies the development of
132 automation macros. This is essential for processing large amounts of data from multiple drill-holes and drill-sites -
133 especially when changes to composite records (splices) are needed.

134

135 **2.2 Image Processing**

136 Ever since IODP Leg 200, core section images have been captured by line scanners as discrete files which
137 are easily loaded into analysis programs with little or no preparation. However, the only access to core images from
138 the first approximately 200 ocean drilling cruises are through digitized photographs of entire cores laid out on a
139 table in parallel sections (FigureFig. 2A). CODD includes a module for cutting core section images from core table
140 photo images, correcting them for uneven lighting, scaling them to mbsf (meters below seafloor) and combining
141 them into a single core image (FigureFig. 2B) through a series of simple steps. In general, the outer 5% of
142 each section image is excluded to minimize friction effects of coring that tend to bend horizontal layers. In practice
143 it takes between 1 and 2 minutes to go from loading a core table photo to producing a scaled composite core image.
144 The visualization and impact of the scaled composite is very much different from the core table photo and of much
145 greater value during data analysis. The use of scaled composite core images has proven to be particularly effective in
146 creating site splices or for the checking of existing splices.

147 Lighting correction is a necessary step when using images cut from core table photos because the light
148 source used for the original photos was co-located with the camera above the center of the core table, resulting in the
149 center of the picture being brighter than the edges (Schaaf and Thurow, 1994; Nederbragt and Thurow, 2001, 2005).
150 This effect is illustrated by profiles of lightness from H S L (hue, saturation, lightness) representations of section
151 images plotted together (FigureFig. 2A inset). For these sections the variability of the intensity of lightness,
152 excepting some spikes representing darker layers, is around 50 units of lightness (out of a full scale of 0 - 255). The
153 difference from the center to the ends of the best-fit line to the profiles is approximately 25 lightness units, so
154 uneven lighting has a significant effect on the section images. When the core table photos are viewed, the observer's
155 eyes and mind make a correction and the uneven lighting seems subtle, but we have found that when stringing
156 section images together to make a composite core image the 1.5 m long lighter/darker cycles are readily apparent.
157 As many ocean drilling sediment cores vary in lightness as a function of carbonate and/or biogenic silica content
158 (e.g. Balsam et al., 1999), lighting cycles in core images degrade the usefulness of core color or lightness profiles as
159 proxies for other properties of interest or for spectral analysis. Thus CODD processing of core table photos includes
160 a step which fits a line to the lightness profiles and then applies a "flattening" filter which brightens the section
161 images away from the center according to the fit. While not perfect, the process removes most of the 1.5 m color
162 cyclicity (FigureFig. 2B). There is also lighting variation across the core box images that can produce a 9/10 m cycle
163 in the spliced composite images. It appears to be somewhat more diffuse than the along-core section variation and
164 hasn't hindered the present work. We are developing a process to correct for lighting variation of the entire core box
165 image prior to cutting the individual section images. This may also allow us to remove the color cast present in
166 many of the older core box images, such as the purplish hue seen in Fig. 2A.

167

168 **2.3 Splicing, Stretching, and Squeezing**

169 In the same manner that sections may be strung together to make a composite core image, extracted splice
170 sections of core images from different holes can be merged into a single scaled spliced site image (FigureFig. 3a).
171 Splicing is a 2 step process, the first of which involves offsetting the mbsf depth for individual cores to a composite
172 depth by aligning features in data collected from multiple holes. It is worth noting here that it is rare that all features

173 in individual cores from different holes align - as coring disturbance (e.g. extension or compression at the top and
174 bottom of piston cores, [see Ruddiman et al. 1987 for an in depth discussion](#)) or natural variability mean that while
175 one feature may align, another is offset (e.g. Lisiecki and Herbert, 2007). The individual setting the splice (the
176 correlator) makes a decision as to which feature to align based on overall considerations of the splicing process.
177 Once the core offsets are set, the correlator chooses tie points between holes to produce as complete a sedimentary
178 record as possible while avoiding any possible duplication. In the past this has been done using data profiles of
179 properties measured on whole round core sections - primarily density from Gamma Ray attenuation (GRA), and
180 magnetic susceptibility (MS) as well as reflectance spectrophotometer intensity (RSC) on split sections. This can
181 prove to be tricky when using data that are replete with similar cycles. Cycle skipping or doubling is a constant
182 source of potential error and the inclusion of images in the process helps greatly. [While checking splices or](#)
183 [splicing cores and choosing tie points we used the same criteria as typically used by the shipboard stratigraphic](#)
184 [correlator for \(IODP expeditions. The splice should contain no coring gaps and disturbed sections are avoided.](#)
185 [Where possible we avoided using the top and bottom ~0.5 m of cores, where disturbance resulting from drilling](#)
186 [artifacts is most likely. Those portions of the recovered core most representative of the overall stratigraphic section](#)
187 [of the site are picked and the number of tie points is minimized to simplify sampling.](#)
188 [number of tie points to](#)
189 [simplify sampling is minimized.](#)

189 An example from Ceara Rise Site 927 demonstrates image utility while examining an existing splice. A 10
190 m long section of images and data is presented in [FigureFig. 3](#). Poor agreement between offset data from all three
191 holes of Site 927 occurs around 50 mcd, immediately below a splice tie in the published splice for the site
192 ([FigureFig. 3A](#)). The images show poor agreement between the light and dark bands in cores 927C-05H and 927B-
193 06H. A better solution is obtained by reducing the offset of 927B-06H by 1.6 m to align the peak in RSC seen
194 around 50.2 mcd in 927C-05H with a similar peak at 51.8 mcd in 927B-06H ([Fig. 3B, 3C](#)). Fortunately, because the
195 core images are depth scaled, CODD allows us to shift and re-splice both core images and all other datasets using a
196 simple algorithm. The resultant shift shows better agreement between images and data from both holes.
197 Significantly, the shift illustrated removes one 40 ka obliquity cycle from the isotope record (Bickert et al. 1997) and
198 will alter a tuned age model accordingly.

199 Traditionally, once the splice has been set, subsequent samples are taken and measurements made only
200 from the core material included in the splice. While three or more holes are often cored at sites devoted to
201 paleoceanographic studies, the volume of samples available within a splice is equivalent to a single hole. And since
202 archival halves of each core are reserved for later sampling, it is often difficult to obtain [new](#) samples along a
203 heavily sampled section of the splice. More material is available from sections of cores not included in the splice,
204 but as mentioned above, the process of aligning and offsetting cores from adjacent holes by matching features is
205 imperfect due to coring effects and natural variability (e.g. Lisiecki and Herbert 2007, Wilkens et al, 2009).
206 Misalignment of off-splice features may add significant noise when in-splice and out-of-splice data are
207 [stackedcombined](#). In order to align features from sections of core not included in the splice it is necessary to
208 stretch/squeeze images and data outside the splice. Magnetic susceptibility data have been stretched from the off-
209 splice data to the splice in [FigureFig. 4](#). [Using CODD, s](#) Sets of tie points between off-splice data and the splice for

210 each hole (yellow numbers in [FigureFig. 4](#)) are selected using cursors. Stretched data and images are updated in real
211 time. The tie points allow investigators to interpolate out-of-splice mcd depths to their equivalent levels in the splice.

212 The ability to squeeze and stretch data and images has a second useful application. Sites drilled in the same
213 general area of the ocean, such as those on the Ceara Rise, often share many physical features in data such as
214 density, magnetic susceptibility, or color in their sediment columns. In a manner similar to the process of stretching
215 and squeezing off-splice data to the splice, CODD employs a cursor driven routine to stretch data and images from
216 different sites to a single common depth scale using similar features. The segment of the stretch of Site 927 to Site
217 926 between tie points 60 and 80 is illustrated in [FigureFig. 5](#). In total, 428 pairs of tie points were identified while
218 matching the upper 304 mcd of Site 927 to the upper 285 mcd of Site 926. Additional constraints such as
219 paleomagnetic reversals and biostratigraphic events may be included, helping to guide the correlation. In practice a
220 user views multiple data types and images simultaneously and tie points selected from one data set are mapped to all
221 others at the same time.

222

223 **2.4 Depth to Age**

224 Once data and images from the individual sites have been tied to a common depth scale the final CODD
225 processing step is to set everything to a single age model. We used the age models of Bickert et al (1997) and
226 Tiedemann and Franz (1997), adjusted for our splice corrections and updated to Laskar et al. (2004), to compare
227 age-scaled images and data from the various Ceara Rise sites. An example comparing Sites 926 and 927 is presented
228 in [FigureFig. 6](#). Comparison of the composite images is remarkable for the fact that individual sedimentary layers
229 that represent sometimes less than 10 kyr are readily identifiable between sites. This suggests that in areas where the
230 sediment has enough color variation highly targeted samples may be collected that represent precisely the same
231 event at multiple sites.

232 MS data and the composite image of Site 926 are compared with orbital calculations using Laskar et al.
233 (2004) in [FigureFig. 7](#). The orbital curve was calculated using 100% of the eccentricity (E) effect plus 50% of the
234 obliquity (T) and precession (P) intensities. Correlation of the MS data to the Laskar model was the primary basis
235 for the Bickert et al_ (1997) and Tiedemann and Franz (1997) age models, so agreement between the 2 curves is
236 expected. They used a correspondence between MS maxima and northern hemisphere summer insolation minima
237 to develop their age models. This phase relationship was found to be most consistent in both precession and
238 obliquity frequency bands (Shackleton and Crowhurst 1997). See Zeeden et al., 2013 for a concise description of
239 their approach. Comparison with a composite core image was not possible for those earlier investigators and our
240 results illustrate the remarkably detailed agreement between cycles seen in the calculations and variations in
241 sediment color. Based on these observations and the well-known phase relationship (Bickert et al. 1997) we
242 refined the tuning for Site 926 from 0-5 Ma tying dark (light) layers, which correspond to MS maxima, to ET-P
243 minima (maxima). We only used only the core image and color reflectance for tuning; therefore plotting the
244 magnetic susceptibility data versus insolation can function serves as a crosscheck for a consistent phase relationship
245 throughout the record.

246

3. Results

We checked the entire splices of Sites 925, 926, 927, 928 and 929 for the last 5 Ma. Most of the changes in the published splice tables were minor although several, such as the one illustrated in [FigureFig. 3](#), were large enough to affect age models based on orbital tuning. Data from samples outside of the revised splices were aligned with the splice based on stretching and squeezing of the out-of-splice data. Mapping pairs to convert depths outside of the splice to the composite depth are provided in supplemental files. For the interval spanning 0 to 5 Ma we compiled 5533 benthic $\delta^{18}\text{O}$ isotope measurements from Bickert et al. (1997), deMenocal et al. (1997), Tiedemann and Franz (1997), Shackleton and Hall (1997), Billups et al (1998) and Tiedemann and Franz (1997). Data were plotted on the updated age model for Site 926. Data from all of the sites are compared with one another and a smoothed curve (Gaussian [smoothingfilter](#)) combining all of the sites is compared to LR04 in [FigureFig. 8](#). Data tables for core offsets, splices, and age models are available as supplemental files to this publication.

Agreement amongst the different Ceara Rise Sites is good in terms of the shapes of the curves while there is a spread in absolute values. This is likely due to the water depths at the different sites, which ranged from 3040 m at Site 925 to 4355 m at Site 929. Offsets in benthic oxygen isotope data between Site 925 and Site 929 in some intervals (e.g. 3.6 to 4.5 Ma) have been suggested to indicate a relatively warmer and saltier NADW than today (Billups et al. 1997).

The overall agreement between the Ceara Rise smoothed composite oxygen isotope curve and the LR04 global compilation is generally quite good although there is a definite difference in absolute values with the Ceara Rise data exhibiting consistently lower values of about 0.2 ‰ than LR04 ([Supplementary Fig. S1](#)). ~~A cross plot of Ceara Rise data and interpolated LR04 values is presented in Figure 9. A line with a slope of 1 and shifted by +0.2 ‰ along the LR04 axis is superimposed on the data, confirming that the offset between the 2 curves is consistent over the entire 5 Myr span of the comparison.~~ The 0.2 ‰ offset is well within the potential regional differences of up to 0.3 ‰ cited by Lisiecki and Raymo (2005). The consistency of the difference over the entire 5 Myr scope of this study is remarkable given the regional mix of data used for LR04.

While the agreement between Ceara Rise and LR04 oxygen isotope data is good, there are discrepancies in some intervals. The 2 curves are out of sync between 1.80 and 1.90 Ma with LR04 exhibiting 2 maxima whereas Ceara Rise contains only 1. As this is close to a point where the LR04 stack switched from Site 677 (0-2 Ma) and ~~92Site 927~~ (0-1.7 Ma) to Site 849 (1.7-3.6 Ma), misalignments in the stack between single sites with the original spliced records could have led to a mismatch here. Tuning for Site 926 in this interval is robust and does not allow a shift that could accommodate the mismatch. Hence the interval from 1.80 and 1.90 Ma in the LR04 stack has to be revised. Even larger differences are seen between 4.0 and 4.5 Ma ([FigureFig. 910](#)). Data from Site 929 have been shifted +0.25 ‰ in [FigureFig. 910](#) to aid in the comparison of the excursions in the data. The data from Sites 925 and 929 are in good agreement, but the Ceara Rise smoothed compilation, which is almost entirely composed of data from the 2 sites over this age interval, bears little resemblance to LR04. As pointed out in Lisiecki and Raymo (2005), their stack prior to 4 Ma includes far fewer sites than the more recent data. The 4.0 to 4.5 Ma interval is also one of low amplitude variability in $\delta^{18}\text{O}$ as a response to orbital variation, making the tuning effort at the individual sites contributing to LR04 more difficult than at later time intervals. Better correlation of data older than 4.5 Ma

284 suggests that age model uncertainties are confined to 4.0 - 4.5 Ma and do not necessarily offset the age models for
285 older sediments in LR04 or our compilation.

286 Assessing uncertainty in the age model is difficult and cannot be discussed in this manuscript as it would
287 require extensive testing. However, in Zeeden et al. (2013) and (2014) this is already done with regards to the
288 uncertainty in the target curve. The outstanding match of sedimentary pattern and insolation calculations, which is
289 amazing, keeping in mind that the Laskar et al. 2004 model is based on a relatively short time of observational data,
290 gives confidence that the error for the Miocene is less than a single precession cycle. Due to the excellent match in
291 patterns we think the main error lies in the accuracy of the target (precession and obliquity). The error in precession
292 maxima and minima positions will be only relevant for times older than 5 Ma (see Lourens et al. 2004), and this is
293 as already discussed in the Zeeden et al. (2013, 2014) papers.

294

295 **5. Discussion**

296 Independent tuning of Site 926 images and physical property data to the Laskar 2004 orbital solution and
297 integration of available benthic stable isotope data from the Ceara Rise provides a new regional reference section for
298 the equatorial Atlantic covering the last 5 million years. Comparing the CODD based new stack from the Ceara Rise
299 to the LR04 stack reveals overall very good agreement suggesting that most of the LR04 stack is robust for the
300 interval from 0-4 Ma. Disagreement in the interval from 1.8-1.9 Ma (FigureFig. 940) points to uncertainties in the
301 records of Sites 677 and 849. The record of Site 677 (Shackleton et al., 1990) has a gap in the composite around this
302 time interval at 85 mcd. Our unpublished re-examination of the Mix et al. (1995) Site 849 age model suggests that it
303 might be affected by issues in the composite record revolving around core 849C 5H at around 52 mcd. Construction
304 of an equatorial Pacific stack, presently underway, should resolve the issue.

305 The differences between LR04 and the Ceara Rise average between 4 and 4.5 Ma reveals a more complex
306 matter that questions assumptions made in LR04. The tuning in Site 926 (FigureFig. 1044) in this interval is robust
307 and can not be changed. The match between the precession-dominated insolation curve and the dark/light pattern
308 shown in the composite site image is excellent. To match the LR04 and the Ceara Rise isotope stacks, the Ceara
309 Rise stack needs to be shifted by 21 kyr to older ages between 4.1 and 4.3 Ma, which is not possible without
310 changing the phase relation between insolation and the dark/light pattern of the Ceara Rise sediments. The LR04
311 stack is basically tuned to obliquity in this interval with lighter $\delta^{18}\text{O}$ in obliquity maxima. The major discrepancy at
312 4.2 Ma occurs in an interval of low obliquity amplitude and higher precession amplitude modulation (FigureFig.
313 1142). Lighter $\delta^{18}\text{O}$ values match insolation maxima in the interval around 4.2 Ma, thus suggesting that the cyclic
314 changes in $\delta^{18}\text{O}$ are related to precession rather than obliquity. Moreover, the minimum in $\delta^{18}\text{O}$ at 4.18 Ma and the
315 maximum at 4.21 Ma in the Ceara Rise stack do not correlate to obliquity minima and maxima as they do before and
316 after this interval, which coincides with a minimum in the 1.2 myr obliquity amplitude modulation. A closer look at
317 the individual isotope records at Ceara Rise (FigureFig. 1243) reveals that these cycles are indeed precession cycles,
318 seen in the site composite image as well as in the benthic $\delta^{18}\text{O}$ data. We therefore conclude that the LR04 stack
319 misinterpreted these two cycles as one obliquity cycle that then was used to tune the LR04 age model. According to
320 the Ceara Rise tuning this interval is not related to obliquity but rather to precession variations. This means that the

321 assumption in LR04 matching all cycles to obliquity is dangerous in intervals of low obliquity amplitude and can
322 lead to incorrect tuning results.

323 Further study of splices and age models used in the data contributing to LR04 will be needed before these
324 discrepancies can be fully resolved. Such clarification is a necessary step in the ongoing effort to create a global
325 correlation of isotope and other data that can be resolved at the isotopic stage level. Such examination of other areas
326 of the oceans will also aid in the development of regional isotope curves to compare with our findings for the Ceara
327 Rise. The CODD approach is a useful tool for extending oxygen isotope reference records into the Miocene and
328 beyond. Combining multiple records from several sites drilled in an oceanic region is greatly facilitated by CODD
329 and helps to form a regional stratigraphic framework. Stacked records from different regions, such as the equatorial
330 Pacific, are urgently needed to test and verify the completeness of each record as gaps can occur on a regional scale.
331 Establishing high resolution age models on a regional scale is the key to understanding paleoceanographic changes
332 on orbital timescales for the entire Cenozoic.

333

334 **6. Conclusions**

335 We have demonstrated a new system for capturing core images as data using newly developed CODD
336 software. The ability to transform core table photos and line-scans of core sections into data as depth or age scaled
337 core images has helped greatly in the task of revising published splices for Ceara Rise sediments cored during ODP
338 Leg 154. Comparison of the revised data with the LR04 global oxygen isotope stack reveals that there are sections
339 of the stack that are not well resolved. Further study of data contributing to LR04 will lead to a clarification of the
340 misfits we have found as well as establishing other regional isotope offsets from a global stack. The CODD software
341 package thus could-can play a key role in the construction of a new generation of the benthic isotope stack and
342 surely will be very helpful in extending the stack into the Miocene. The next important step will be to form a more
343 robust and accurately tuned initial signal used to form the benthic isotope stack.

344

345 **Acknowledgements**

346 Development of CODD was partially supported by post cruise funds from U.S. Science Support for RW.
347 Financial support for this research was also provided by the Deutsche Forschungsgemeinschaft (DFG) to TW and
348 AJD.

349

350

350

351 **References**

352 Bickert, T., Curry, W. B. and Wefer G.: Late Pliocene to Holocene (2.6– 0 Ma) western equatorial Atlantic deep-
353 water circulation: Inferences from benthic stable isotopes, Proc. Ocean Drill. Program Sci. Results, 154, 239–
354 254.1997.

355

356 Bickert, T., G. H. Haug, and R. Tiedemann: Late Neogene benthic stable isotope record of Ocean Drilling Program
357 Site 999: Implications for Caribbean paleoceanography, organic carbon burial, and the Messinian Salinity Crisis,
358 Paleoceanography, 19, PA1023, doi:10.1029/2002PA000799, 2004.

359

360 Billups, K., Ravelo, A.C. and Zachos, J. C.: Early Pliocene deep water circulation in the western equatorial Atlantic:
361 Implications for high-latitude climate change, Paleoceanography, 13, 84–95,1998.

362

363 deMenocal, P., Archer, D. and P. Leth: Pleistocene variations in deep Atlantic circulation and calcite burial between
364 1.2 and 0.6 Ma: a combined data-model approach, in Shackleton, N.J., Curry, W.B., Richter, C., and Bralower, T.J.
365 (Eds.), Proc. of the Ocean Drilling Program, Scientific Results, Vol. 154, 285-298,
366 doi:10.2973/odp.proc.sr.154.113.1997.

367

368 Drury, A.J., Westerhold, T., Frederichs, T., Wilkens, R., Channell, J., Evans, H., John, C., Lyle, M., and ~~Fain~~Tian,
369 J.: Late Miocene time scale reconciliation: accurate orbital calibration from a deep-sea perspective,
370 Paleoceanography, in press, 2016.

371

372 Hagelberg, T, Shackleton, N., Pisias, N., and Shipboard Scientific Party,: Development of composite depth sections
373 for Sites 844 through 854, In Mayer, L., Pisias, N., Janecek, T, et al., Proc. ODP, Init. Repts., 138 (Pt.1): College
374 Station, TX (Ocean Drilling Program), 79 85, doi:10.2973/odp.proc.ir.138.105.1992.

375

376 Hays, J.D., Imbrie, J. and Shackleton, N.J.: Variations in the Earth's orbit: Pacemaker of the ice ages., Science, 194,
377 1121-1132, doi:10.1126/science.194.4270.1121, 1976.

378

379 Khélifi, N., Sarnthein, M., and Naafs, B. D. A.: Technical note: Late Pliocene age control and composite depths at
380 ODP Site 982, revisited: Clim. Past, v. 8, p. 79-87, 2012.

381

382 Laskar, J., Robutel, P., Joutel, F., Gastineau, M., Correia, A., and Levrard, B.: A long-term numerical solution for
383 the insolation quantities of the Earth, Astron. Astrophys.: 428, 261–285, doi:10.1051/0004-6361:20041335, 2004.

384

385

386 Laskar, J., Fiengo, A., Gastineau, M., and Manche H.: La2010: a new orbital solution for the long-term motion of
387 the Earth, *Astron & Astrophys*, 532, A89, pp. 15, doi:10.1051/0004-6361/201116836, 2011.

388

389 Lawrence, K. T., Bailey, I., and Raymo, M. E.: Re-evaluation of the age model for North Atlantic Ocean Site 982
390 and arguments for a return to the original chronology: *Clim. Past*, v. 9, no. 5, p. 2391-2397, 2013.

391

392 Lisiecki, L. and Raymo, M.: A Pliocene-Pleistocene stack of 57 globally distributed benthic $\delta^{18}\text{O}$ records,
393 *Paleoceanography*, 20, PA1003, doi:10.1029/2004PA001071, 2005.

394

395 Lourens, L., Hilgen, F., Shackleton, N., Laskar, J. and Wilson D.: The Neogene Period, in *A Geologic Time Scale*,
396 edited by F. Gradstein, J. Ogg, and A. Smith, pp. 409–440, Cambridge Univ. Press, Cambridge, 2004.

397

398 Mix, A. C., Pisias, N. G., Rugh, W., Wilson, J., Morey, A. and Hagelberg T. K.: Benthic foraminifer stable isotope
399 record from Site 849 (0–5 Ma): Local and global climate changes, *Proc. Ocean Drill. Program Sci. Results*, 138,
400 371–412, 1995.

401

402 [Nederbragt, A.J., Thurow, J.W., 2005. Digital sediment colour analysis as a method to obtain high resolution climate](#)
403 [proxy records, in: Francus, P. \(Ed.\), Image Analysis, Sediments and Paleoenvironments, Developments in](#)
404 [Paleoenvironmental Research. Springer Netherlands, pp. 105–124.](#)

405

406 [Nederbragt, A.J., Thurow, J.W., 2001. A 6000 yr varve record of Holocene climate in Saanich Inlet, British](#)
407 [Columbia, from digital sediment colour analysis of ODP Leg 169S cores. *Mar. Geol.* 174, 95–110.](#)
408 [doi:10.1016/S0025-3227\(00\)00144-4](#)

409

410 [Ruddiman, W.F., Cameron, D., Clement, B.M., 1987. Sediment disturbance and correlation of offset holes drilled](#)
411 [with the hydraulic piston corer - Leg 94. *Initial Rep. Deep Sea Drill. Proj.* 94, 615–634.](#)

412

413 Shackleton, N. J., Berger, A. and Peltier W. R.: An alternative astronomical calibration of the Lower Pleistocene
414 timescale based on ODP Site 677, *Trans. R. Soc. Edinburgh Earth Sci.*, 81, 251–261, 1990.

415

416 Shackleton, N.J., Crowhurst, S.J.: Sediment fluxes based on an orbitally tuned time scale 5 Ma to 14 Ma, Site 926.
417 In: Curry, W.B., Shackleton, N.J., Richter, C., Bralower, T. (Eds.), *Proceedings of the ODP, Scientific Results*, vol.
418 154. Ocean Drilling Program, College Station, TX, pp. 69–82, 1997.

419

420 Shackleton, N. and Hall, M.: The late Miocene isotope record, Site 926, in Shackleton, N.J., Curry, W.B., Richter,
421 C., and Bralower, T.J. (Eds.), *Proc. of the Ocean Drilling Program, Scientific Results*, Vol. 154, 1997.

422

423 Tiedemann, R., and Franz, S. O.: Deepwater circulation, chemistry, and terrigenous sediment supply in the
424 equatorial Atlantic during the Pliocene, 3.3– 2.6 Ma and 5– 4.5 Ma, *Proc. Ocean Drill. Program Sci. Results*, 154,
425 299– 318, 1997.

426

427 Venz, K. A., and Hodell, D. A.: New evidence for changes in Plio-Pleistocene deep water circulation from Southern
428 Ocean ODP Leg 177 Site 1090, *Palaeogeogr. Palaeoclimatol. Palaeoecol.*, 182, 197– 220, doi:10.1016/S0031-
429 0182(01)00496-5, 2002.

430

431 Venz, K.A., Hodell, D.A., Stanton, C., and Warnke, D.A.: A 1.0 Myr record of glacial North Atlantic Intermediate
432 Water variability from ODP Site 982 in the Northeast Atlantic. *Paleoceanography*, 14, 42–52,
433 doi:10.1029/1998PA900013, 1999.

434

435 Westerhold, T., Röhl, U., Pälike, H., Wilkens, R., Wilson, P.A., and Acton, G.: Orbitally tuned timescale and
436 astronomical forcing in the middle Eocene to early Oligocene, *Clim. Past.*, 10, 955-973, doi:10.5194/cp-10-955-
437 2014, 2014.

438

439 Wilkens, R.H., Niklis, N., and Frazer, M.: Data report: digital core images as data: an example from IODP
440 Expedition 303. *In* Channell, J.E.T., Kanamatsu, T., Sato, T., Stein, R., Alvarez Zarikian, C.A., Malone, M.J., and
441 the Expedition 303/306 Scientists, *Proc. IODP*, 303/306: College Station, TX (Integrated Ocean Drilling Program
442 Management International, Inc.). doi:10.2204/iodp.proc.303306.201.2009.

443

444 Zeeden, C., Hilgen, F. J., Westerhold, T., Lourens, L., Röhl, U., and Bickert, T.: Revised Miocene splice,
445 astronomical tuning and calcareous plankton biochronology of ODP Site 926 between 5 and 14.4 Ma,
446 *Paleogeography, Paleoclimatology, Palaeoecology*, 369, 430-451, dx.doi.org/10.1016/j.palaeo.2012.11.009, 2013.

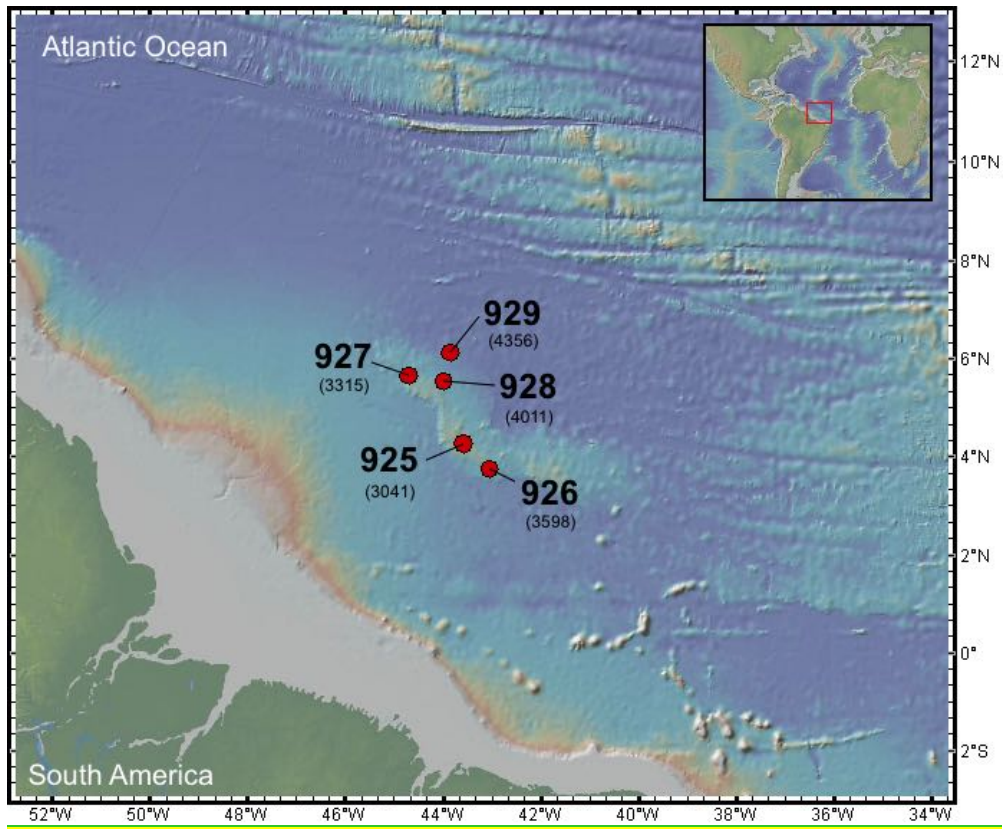
447

448 [Zeeden, C., Hilgen, F. J., Hüsing, S. K., and Lourens, L. L.: The Miocene astronomical time scale 9–12 Ma: New](#)
449 [constraints on tidal dissipation and their implications for paleoclimatic investigations, *Paleoceanography*, 29,](#)
450 [2014PA002615, 10.1002/2014PA002615, 2014201](#)

451

452

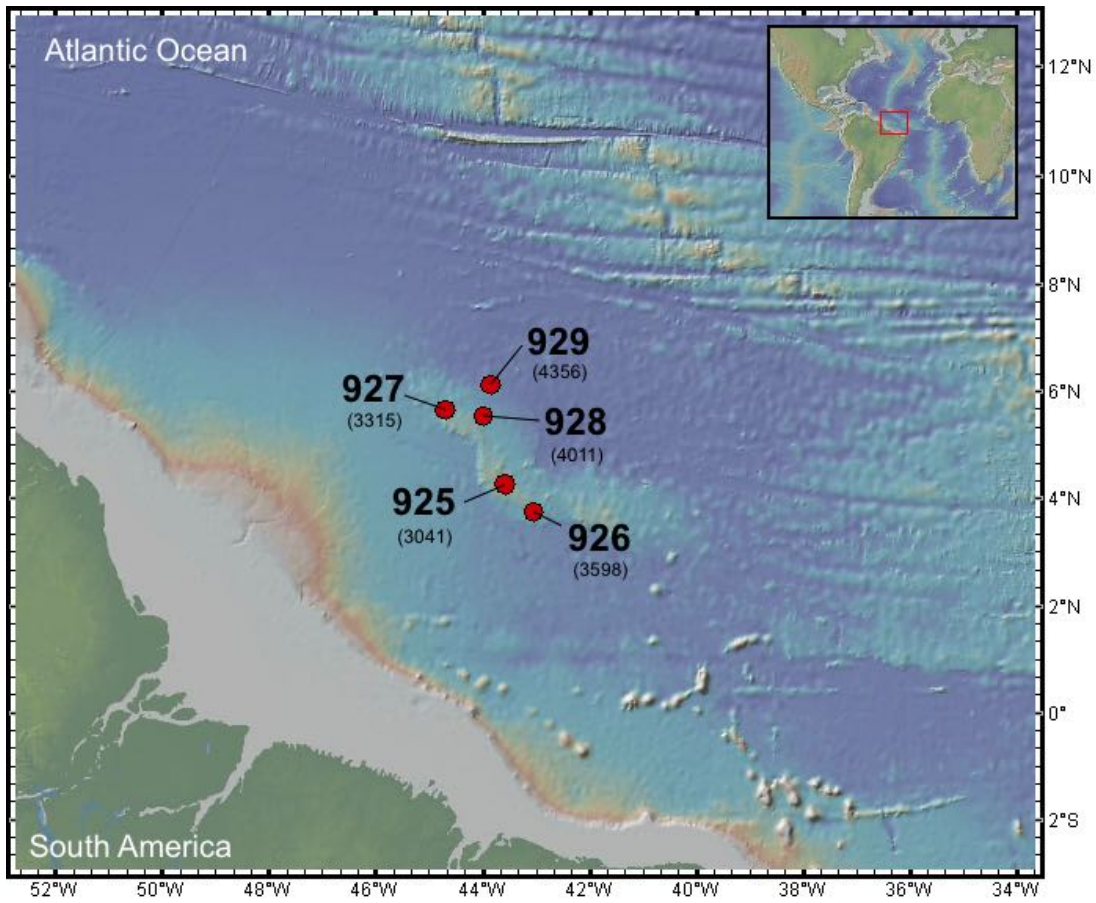
452



453

454

455

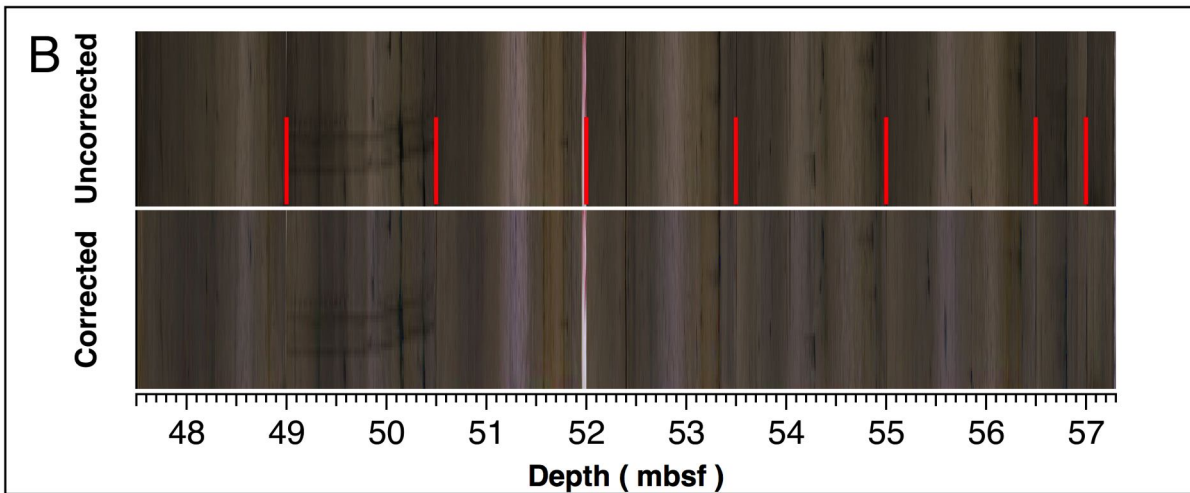
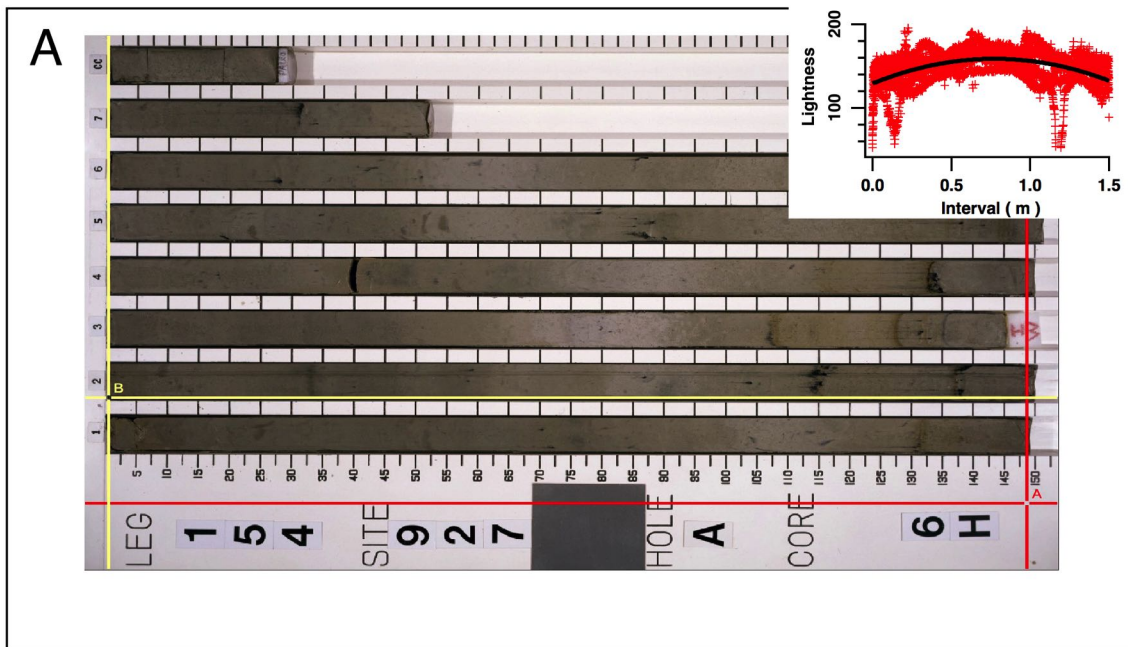


455

456

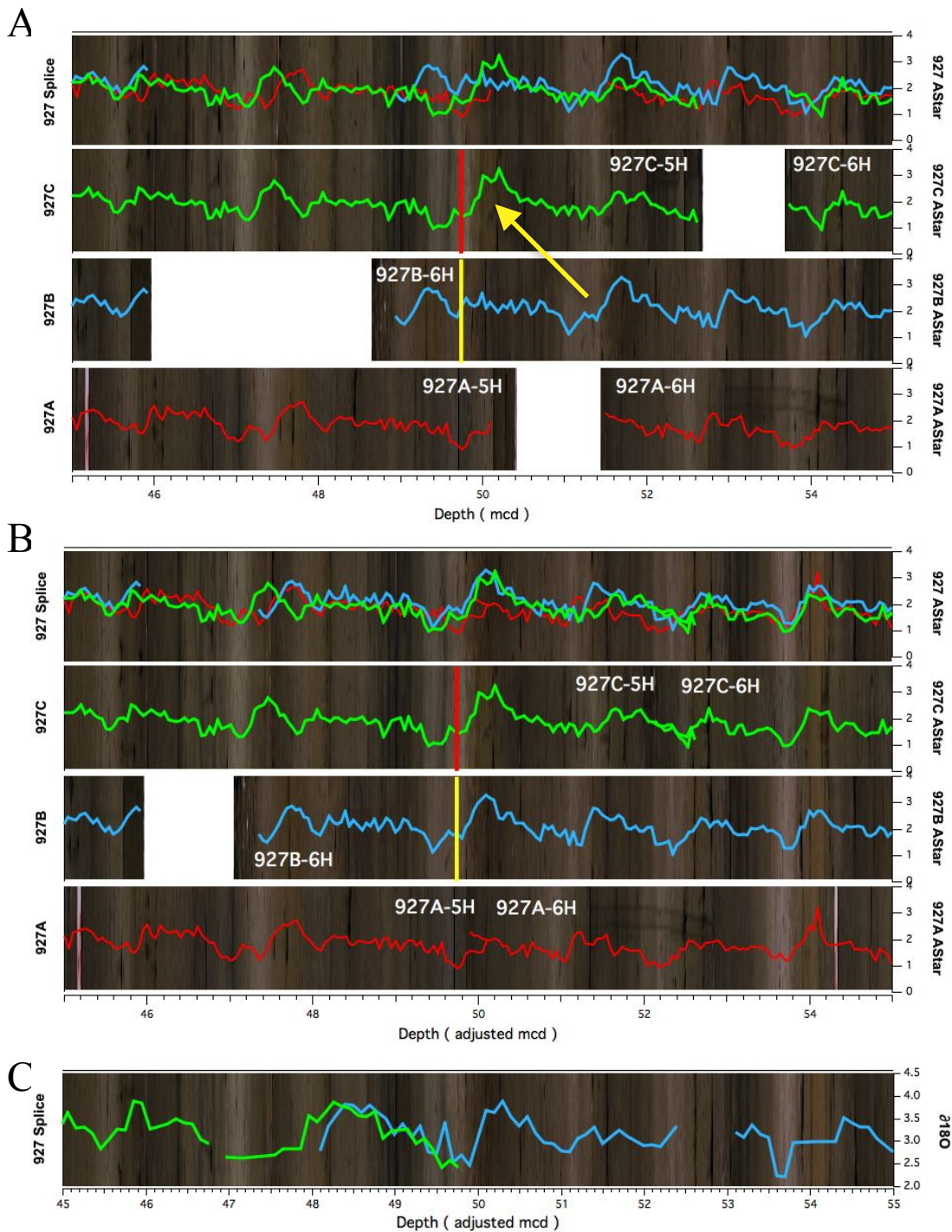
457 **Figure 1: The location of ODP Leg 154 Sites.**

458



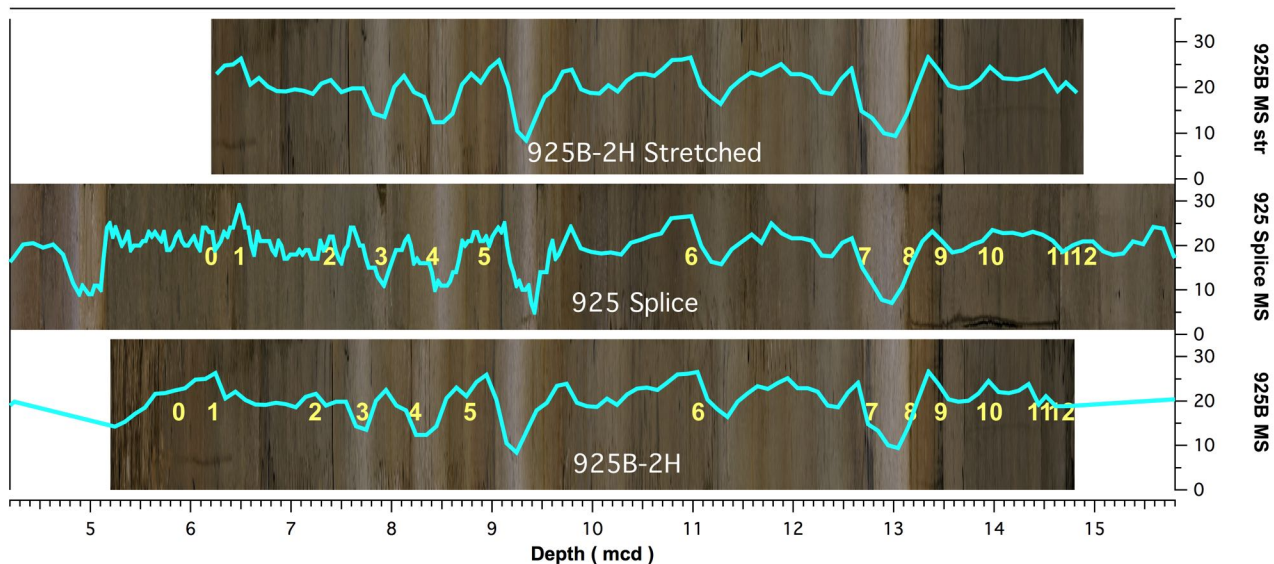
458
 459
 460 Figure 2: Creating a composite core image from a core table image. (A) Image loaded into IGOR. Red cursor moves horizontally
 461 to set bottom locations in pixels of each section. Yellow cursor moves horizontally and vertically to the lower left corner of each
 462 section before cutting. Inset - Lengthwise lightness profiles for each of the cut sections and a best fit line used for the lighting
 463 correction. (B) Composite core image scaled to mbsf. Vertical red lines indicate section breaks. Lower image has been corrected
 464 for uneven lighting in the core box photo.

465
466
467

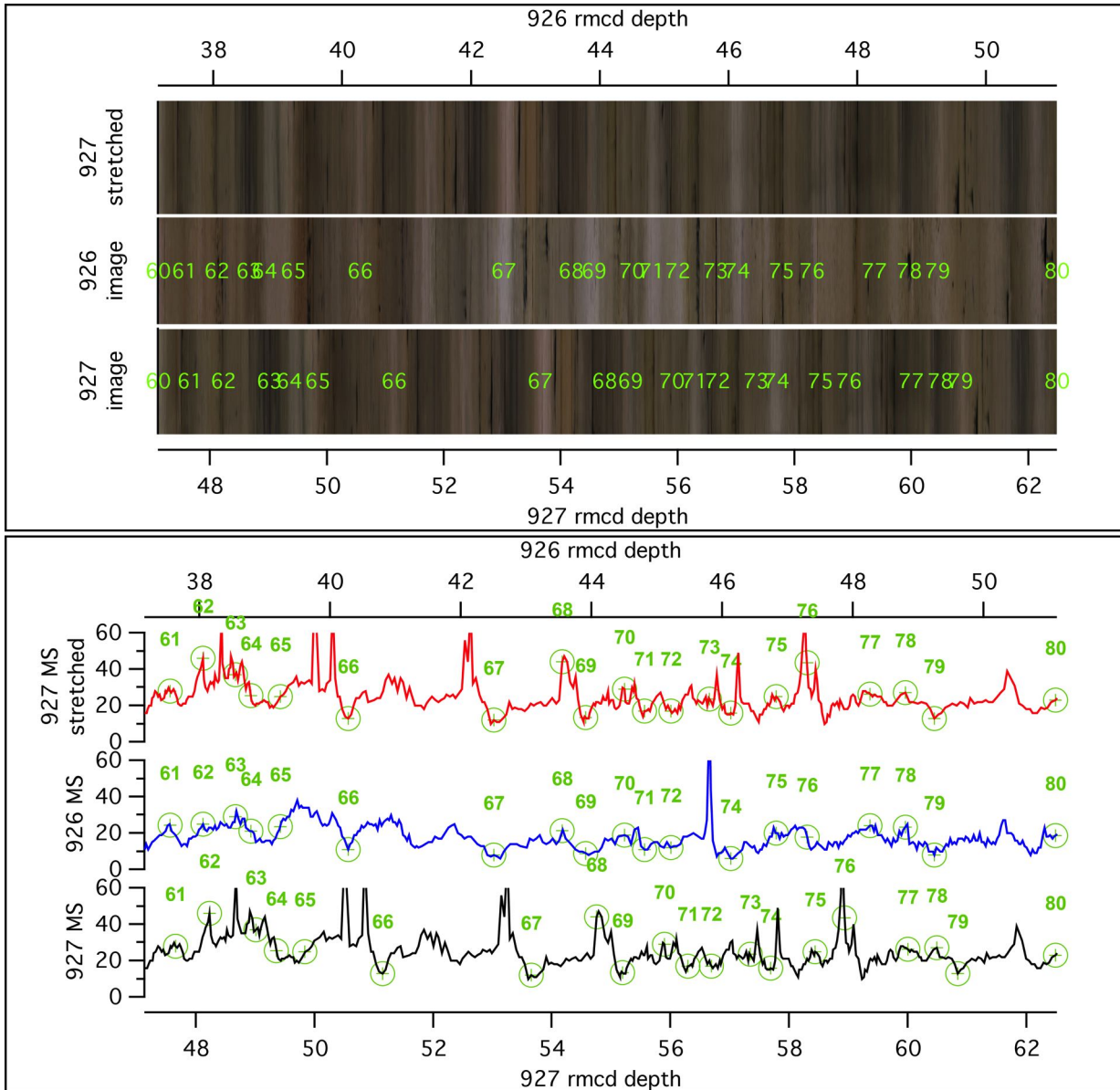


467

468 **Figure 3: A. Reflectance spectrophotometer (RSC) a* data (LAB color model) and core images plotted against the**
 469 **published splice mcd. The yellow arrow indicates misaligned features. The yellow vertical line represents the top of a**
 470 **splice section and the vertical red line shows the bottom of the previous splice section. B. The revised splice. The splice**
 471 **goes from Core 927C-05H to 92Core 927B-06H in both cases, but the offset for 92Core 927B-06H has been reduced by 1.6**
 472 **m in the revised splice to account for the repeat sampling of a cycle. Note the poor agreement of the data between 49 and**
 473 **473 51 mbsf in the original splice. C. Benthic $\delta^{18}O$ revised. Samples were collected based on the original splice, resulting in**
 474 **data duplication between 48 and 50 m adjusted mcd.**

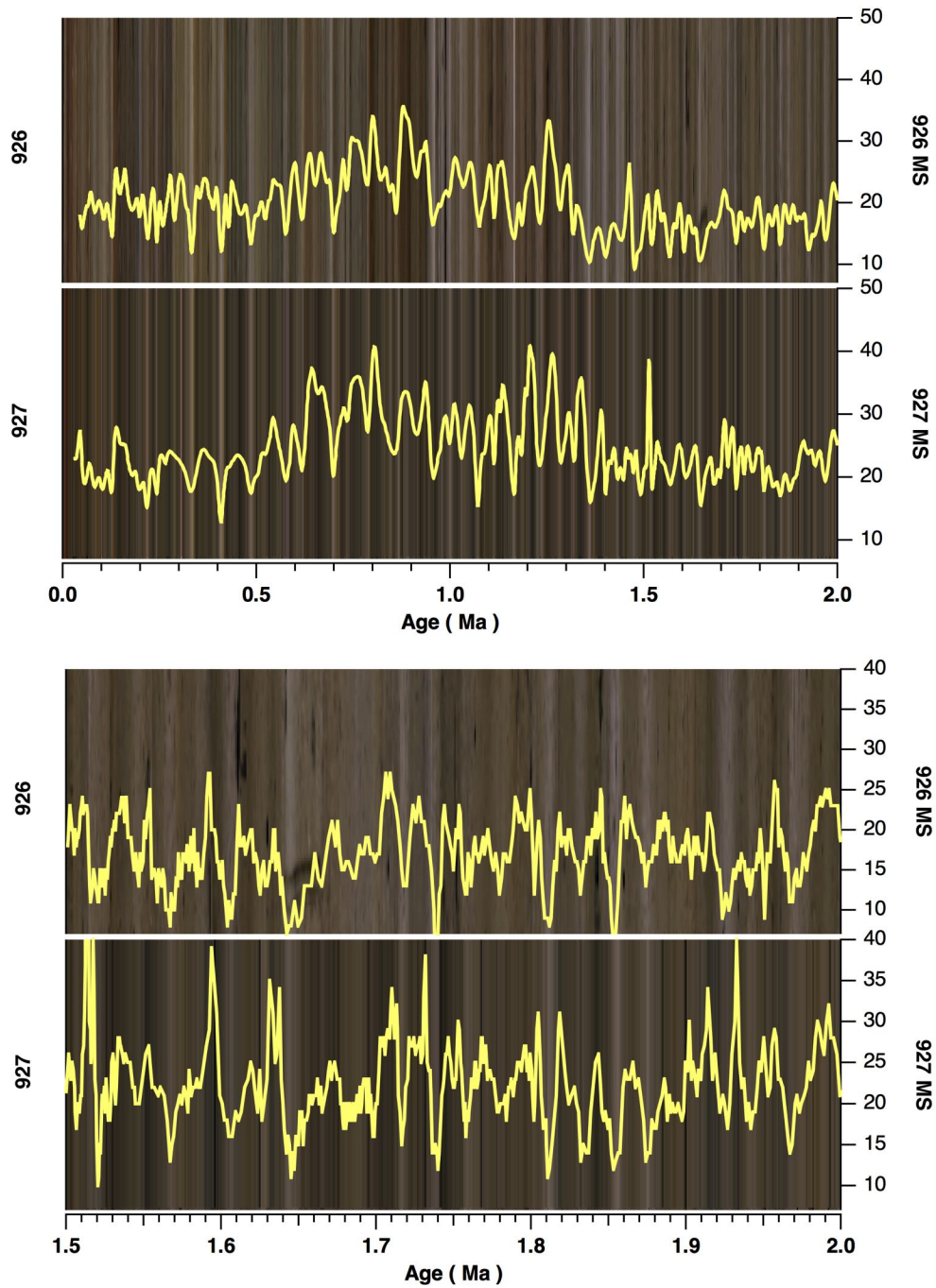


478 **Figure 4: Core 925B-2H was not used for the Site 925 splice and while there is good alignment between the core image**
479 **and data and the spliced image and data at 13-14 mcd, shallower portions of the core are not well aligned with the splice.**
480 **Yellow numbers indicate tie points used to stretch the image and data so that they are in better agreement with the splice.**
481 **Choice of tie points is cursor driven and stretching can be recalculated in real time.**



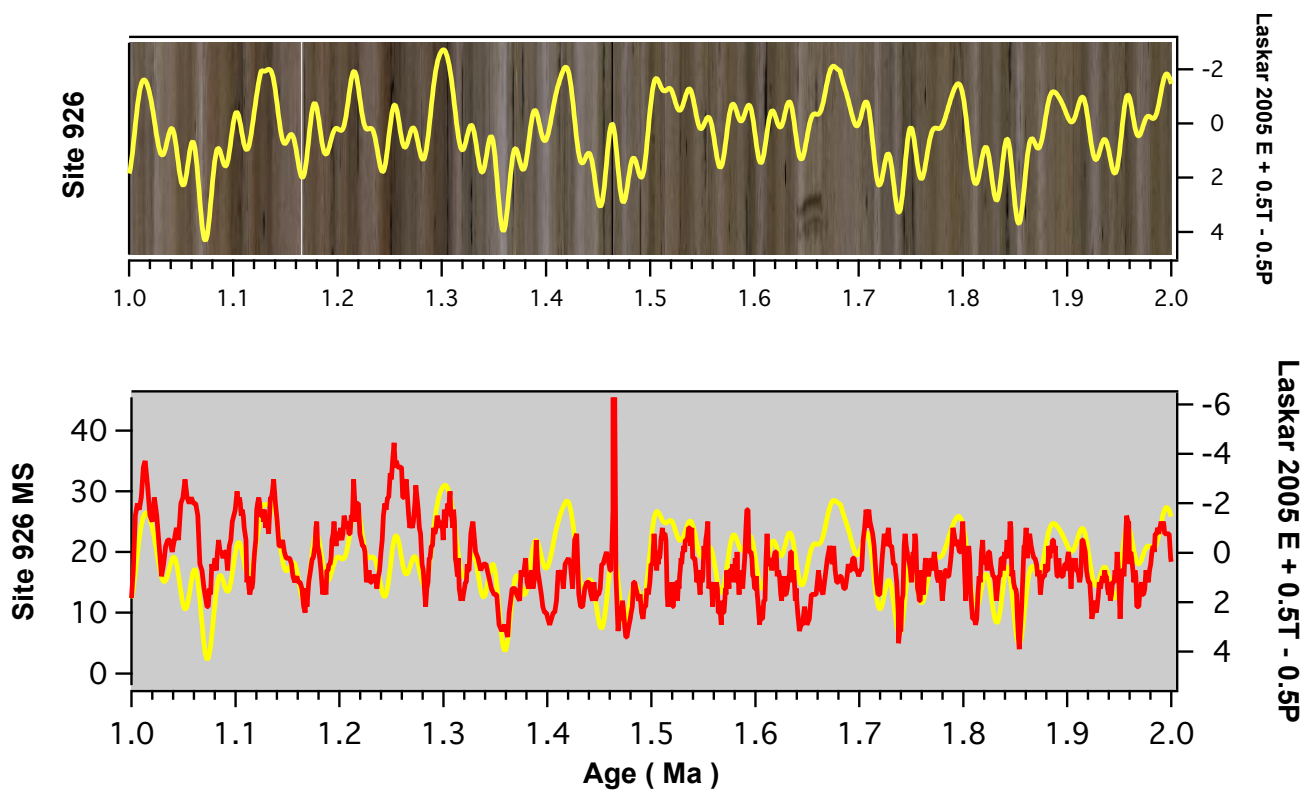
483
 484
 485
 486
 487
 488
 489

Figure 5: Spliced images and MS data from ODP Sites 926 and 927. The rmcd depth scales indicate that there have been small adjustments to the published splices for each site. Site 927 data and image are plotted versus the Site 927 depth scale on the bottom of each graph and versus the Site 926 depth scale at the top. Green numbers indicate tie points between the sites used to stretch the site 927 image and data.

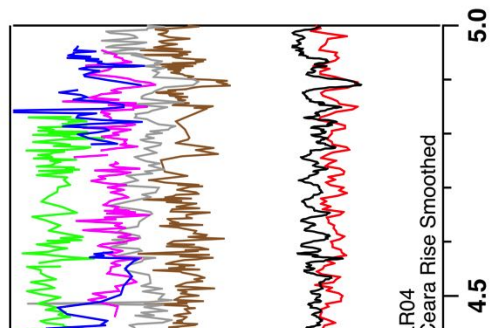
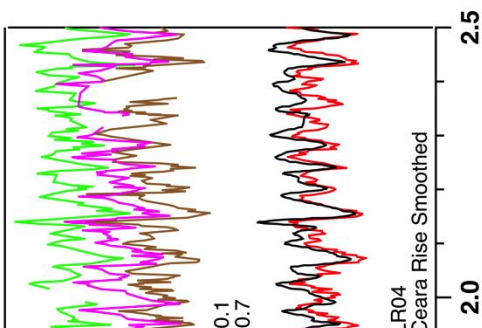
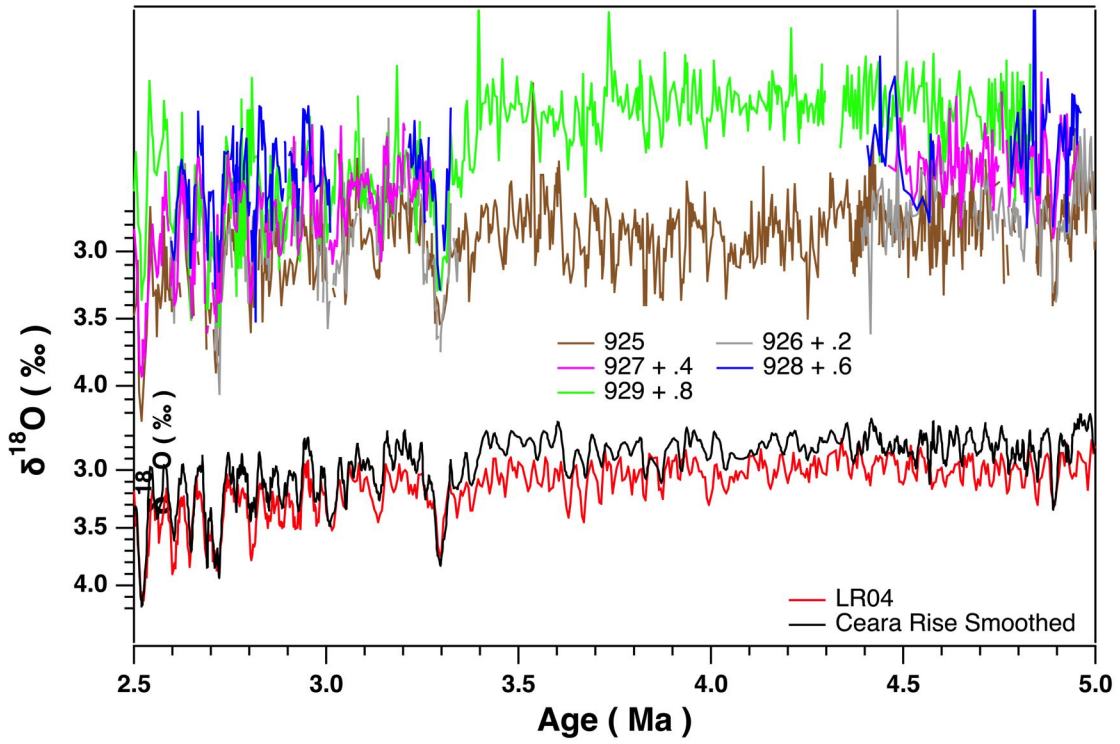
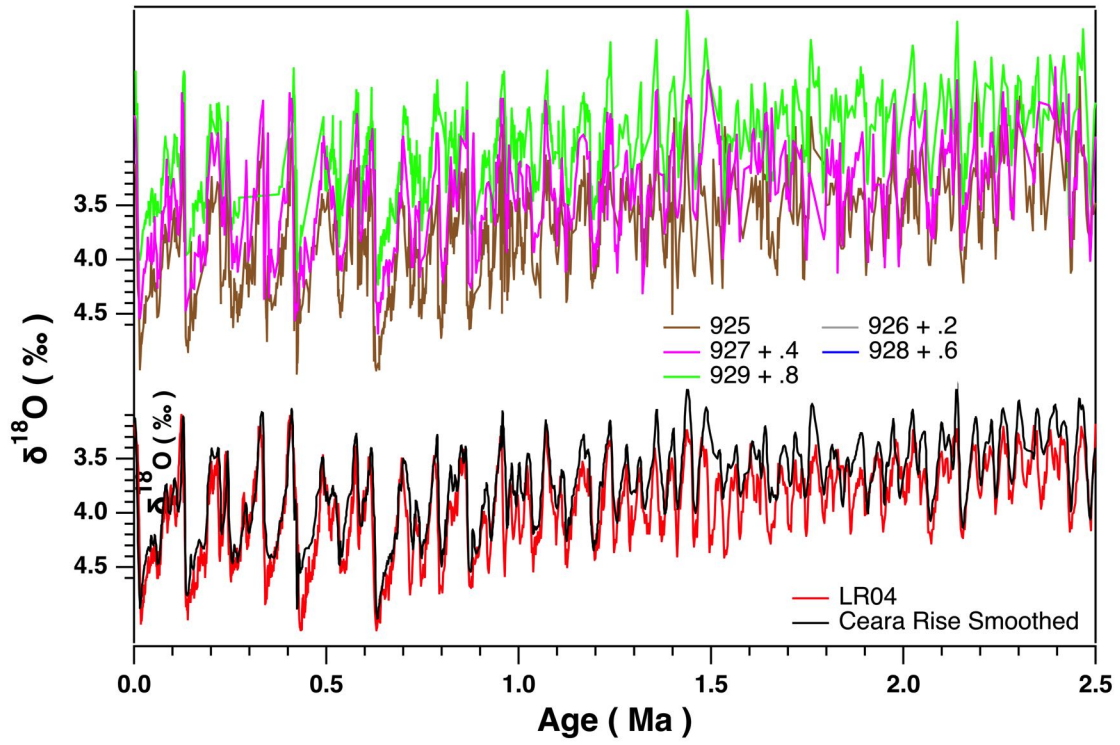


489
 490
 491
 492

Figure 6: Top - Smoothed MS data and images plotted versus age from 0 - 2 Ma. Bottom - 1.5 - 2 Ma detail using non-smoothed data. Fine layers, on the order of 10 kyr, are correlated between Sites 927 and 926.



493
 494
 495 **Figure 7: Laskar et al. (2005) orbital calculation compared to the Site 926 composite image and MS data. E = the effect**
 496 **of eccentricity, T = tilt (obliquity), and P = precession.** The Laskar curve was compared to MS to ~~formulate~~check the
 497 age model used in this study that was based on the images and color reflectance. The composite image is the result of
 498 comparing multiple data sets and individual core images.
 499



501 | **Figure 8: Benthic oxygen isotope data from all Ceara Rise sites compared with one another and a smoothed composite of**
502 **all data compared to LR04. Top - 0 to 2.5 Ma, bottom 2.5 to 5 Ma. Note the $\delta^{18}\text{O}$ scale change between top and bottom**
503 **plots. Individual site traces have been offset as indicated in the legend.**

504

505 Original Figure 9 was removed.

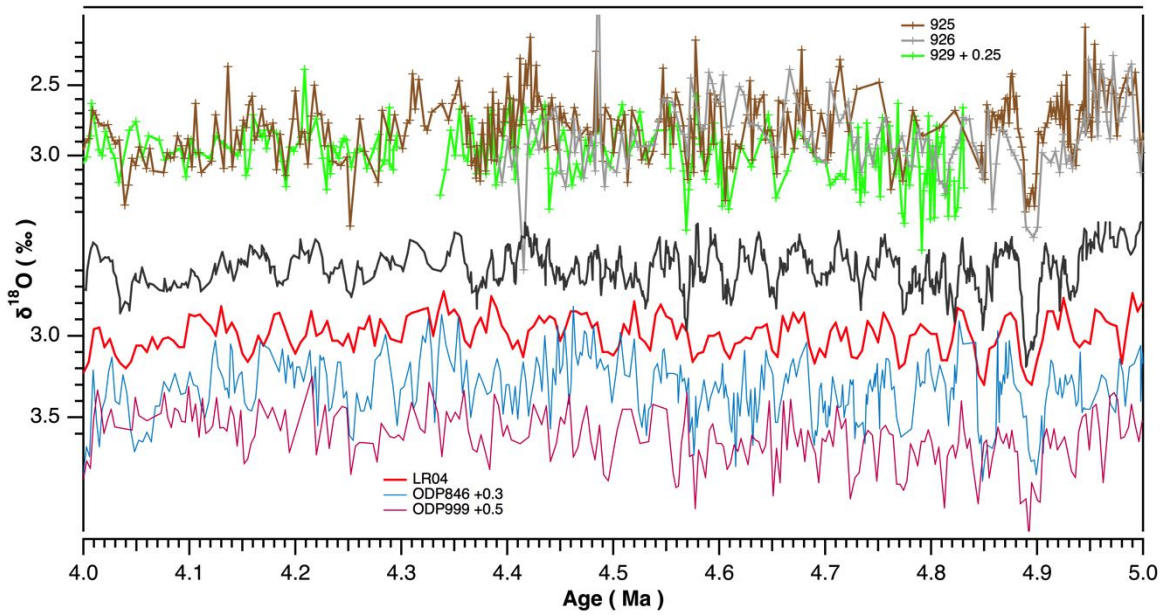
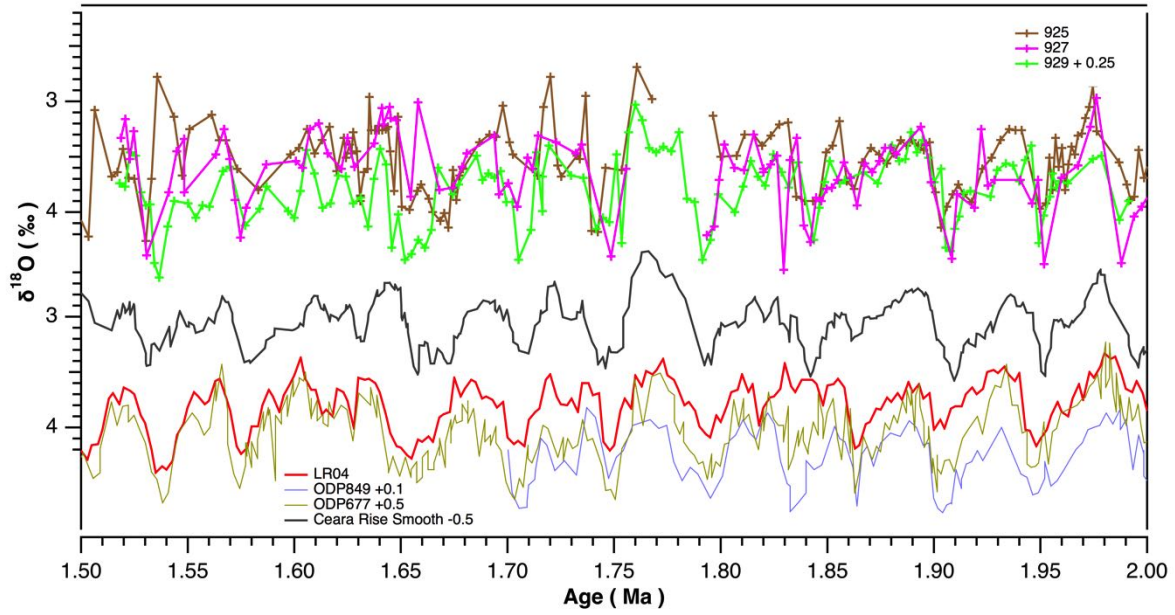
506

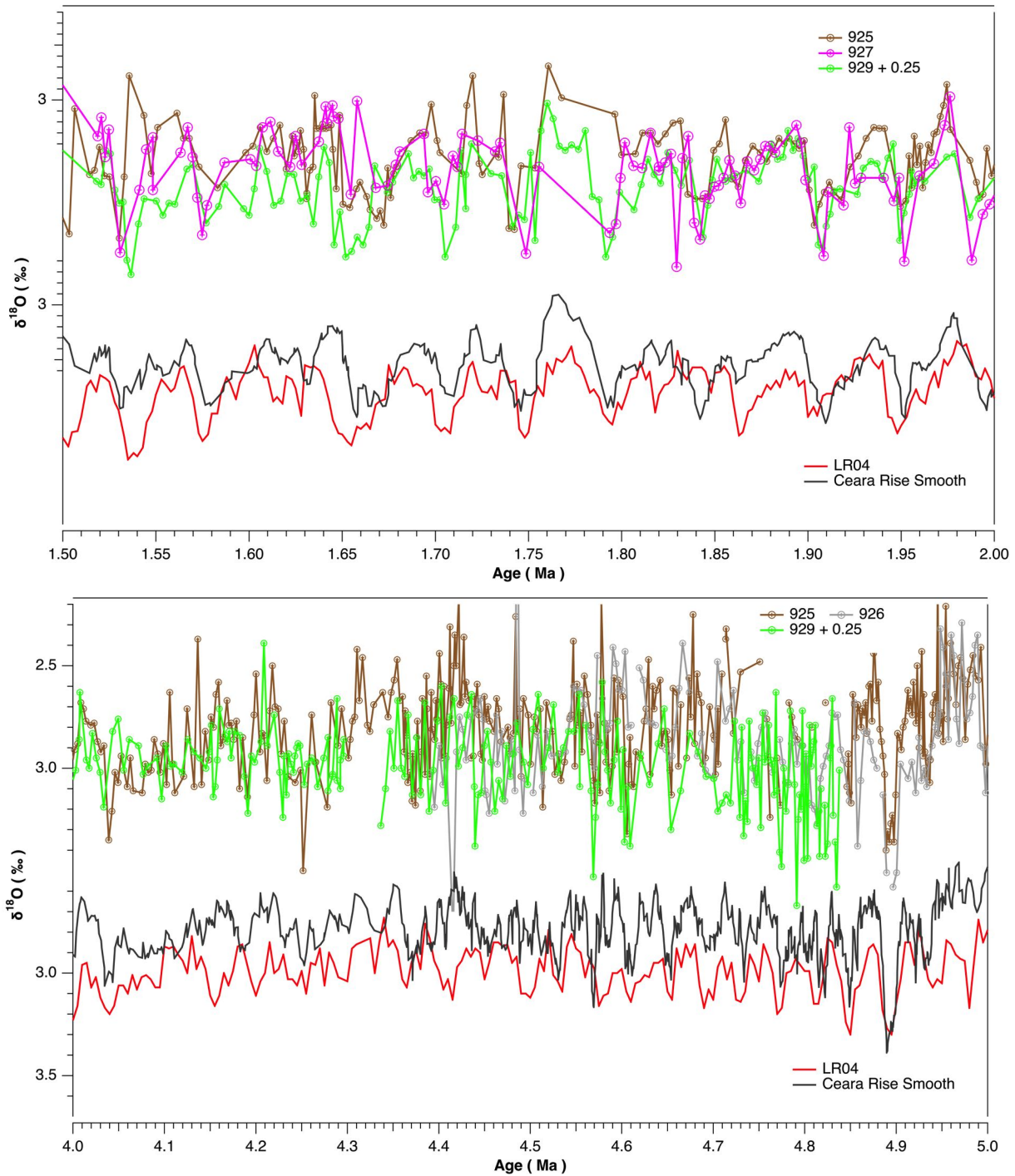
507 ~~Figure 9: A comparison between the oxygen isotope data from the smoothed Ceara Rise composite and the~~

508 ~~LR04 global compilation. The black line represents a 1:1 correspondence that has been shifted by +0.2 ppm~~

509 ~~along the LR04 axis.~~

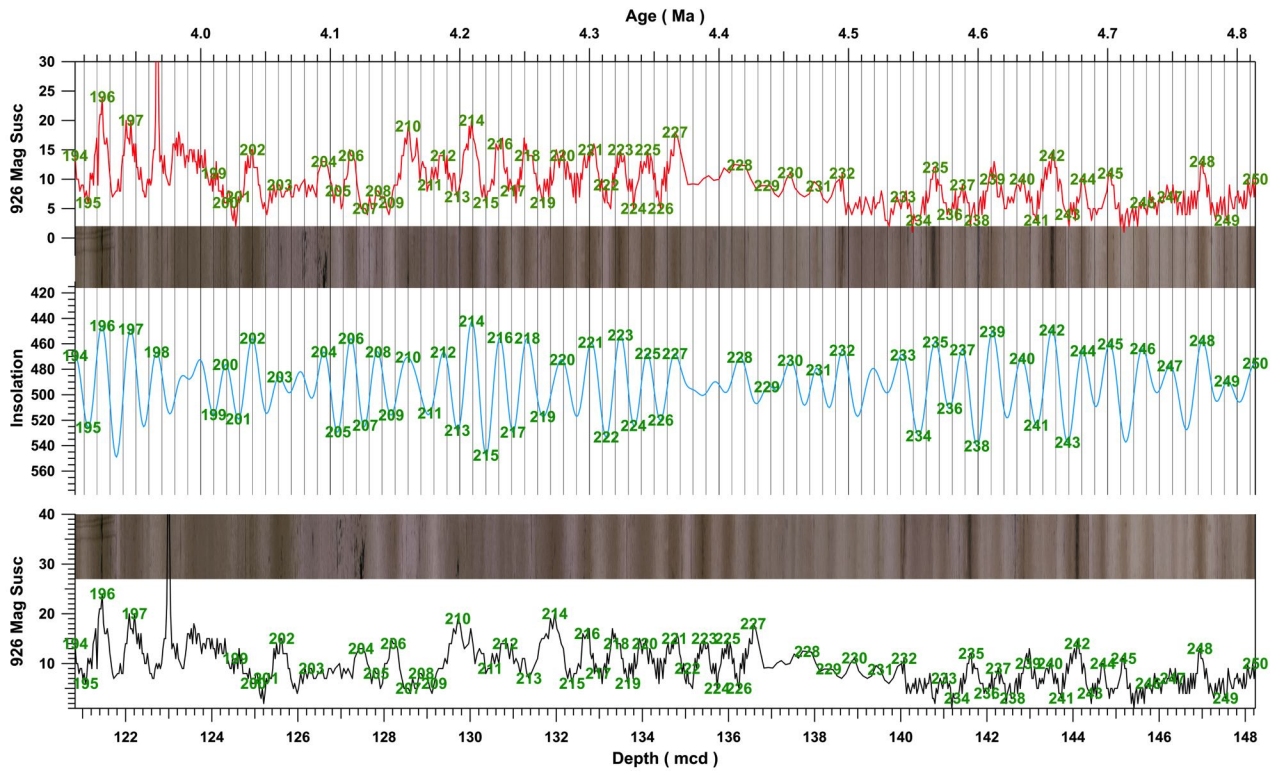
510



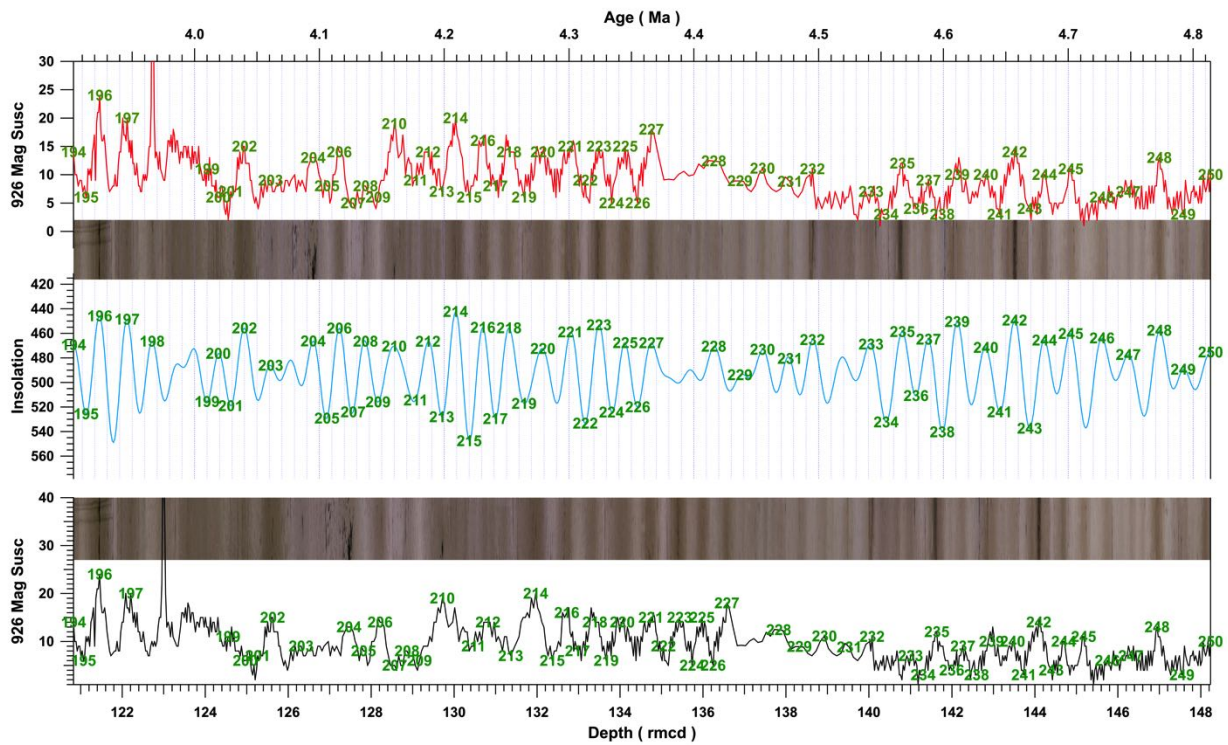


512 **Figure 109:** Detail from **Figure Fig. 8** comparing individual holes to one another and a smoothed composite to LR04 **for**
513 **the intervals 1.5 to 2.0 Ma and 4.0 to 5.0 Ma. For better illustration we plotted the initial alignment target records of the**
514 **LR04 stack. For the 1.5 to 2.0 Ma interval these are the records from ODP Sites 677 and 849, for the interval 4.0 to 5.0**
515 **Ma these are the records from ODP Sites 846 and 999. Some records have been shifted as indicated in the figure for better**
516 **comparison of the data with each other. Note the differences between LR04 and the Ceara Rise average at 1.80 - 1.85 Ma**
517 **although the initial alignment targets are more similar to the Ceara Rise smooth. Also note the difference between 4.0 and**
518 **4.5 Ma. The Site 999 record is from a single hole and the splice of the Site 846 record might be erroneous. The age model**
519 **for the Ceara Rise is very robust in this interval (see. Fig. 10) pointing to potential inconsistencies in the age model**
520 **construction of the Site 846 and Site 999 records.**

521 ~~The Site 929 data have been shifted by +0.25 ppm to better illustrate the agreement of variations between Site 929 and~~
522 ~~Site 925. Site 925 was at a water depth of 3040 m while the depth at Site 929 was 4355 m. The difference in temperature or~~
523 ~~perhaps water masses may be responsible for the baseline offset over this age interval. Note differences between LR04~~
524 ~~and the Ceara Rise average at 1.80 – 1.85 Ma and between 4.0 and 4.5 Ma.~~



525

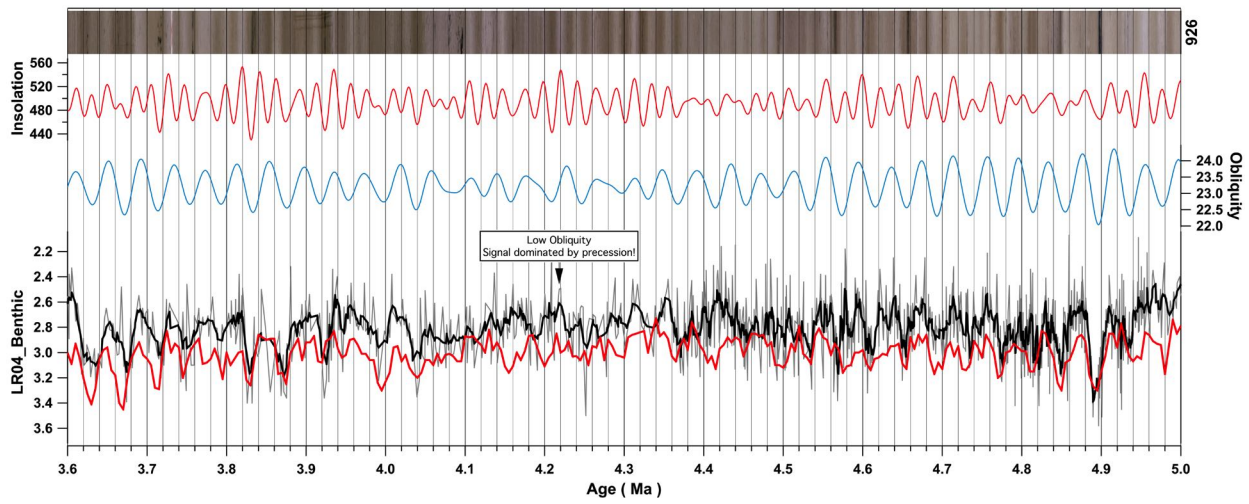


526

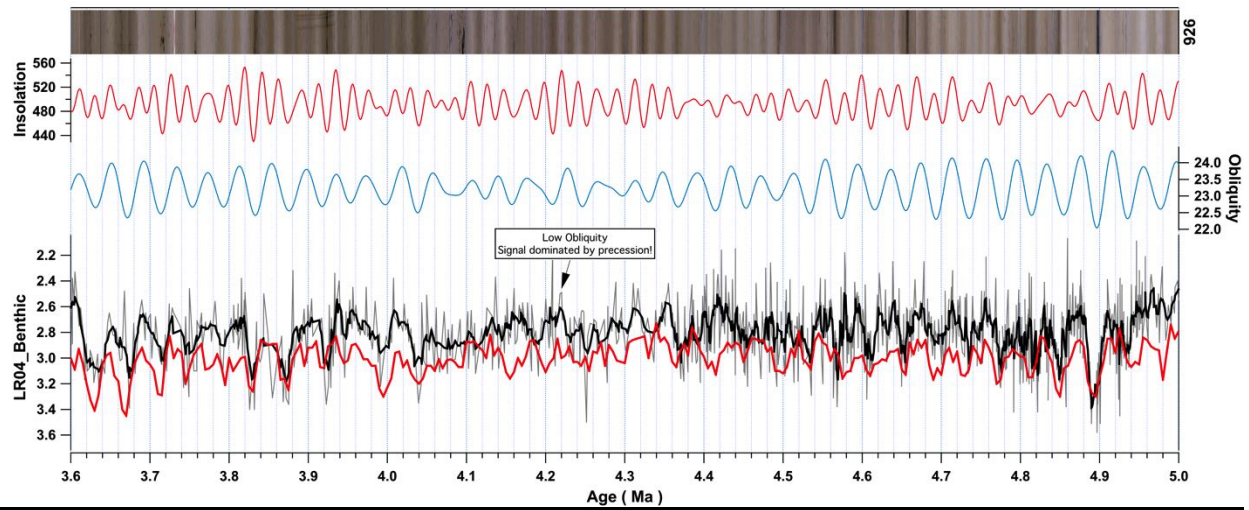
527 **Figure 4110:** Detail from CODD tuning of **92Site 926** magnetic susceptibility and core images to insolation.

528 **Bottom** is data versus depth, **middle** shows insolation 65°N 21st June inverted, **and top** shows image and

529 | magnetic susceptibility versus tuned age. Green numbers mark position of tie points. Numbers identify tie
530 | points between the data and the insolation curve. Light/dark layering in the composite core image is tied to
531 | precession cycles prominent in the insolation curve.
532 |

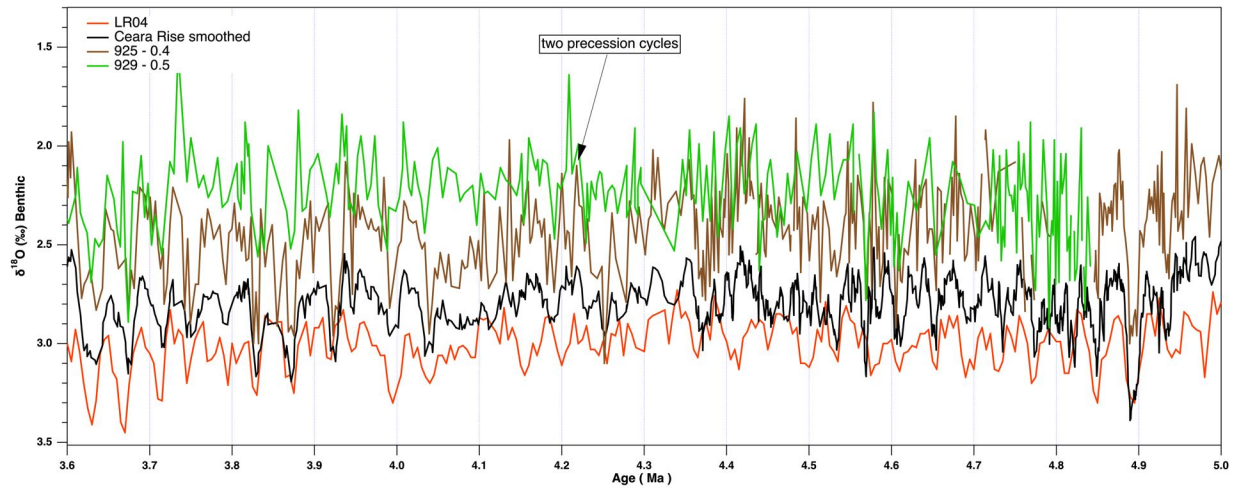


532



533

534 **Figure 4211:** A comparison of LR04 (Red) to Ceara Rise (grey and black (smooth)) to obliquity and insolation from
 535 Laskar et al. 2004. Note that the interval 4.0 and 4.5 Ma exhibits poorly defined obliquity cycles leaving insolation
 536 dominated by precession.



537

538

539 **Figure 1312:** A comparison of LR04 and Ceara Rise (smooth) to 92Site 925 and 92Site 929 benthic isotope data. LR04
 540 assignment of variability in the interval from 4.0 to 4.5 Ma to precessionprecession peaks may have resulted in the
 541 mismatch with the Ceara Rise stack.

543

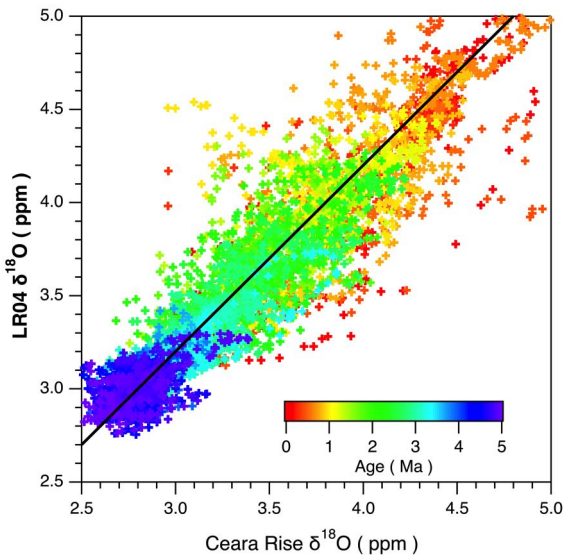


Figure S1: A comparison between the oxygen isotope data from the smoothed Ceara Rise composite and the LR04 global compilation. The black line represents a 1:1 correspondence that has been shifted by +0.2 ppm along the LR04 axis.

566

567 [IGOR CODD Functions, a User Guide, and Help files may be downloaded at www.CODD-Home.net.](http://www.CODD-Home.net)

568

569 [Data Tables may be found on the PANGAEA database at https://doi.pangaea.de/10.1594/PANGAEA.870873.](https://doi.pangaea.de/10.1594/PANGAEA.870873)

570 The tables include:

571 For each site

572 Offset table

573 Splice interval table

574 Spliced magnetic susceptibility (MS) data including Site 926 equivalent depths

575 Isotope data including Site 926 equivalent depths

576 Age model including Site 926 equivalent depths

577 Stretching tie points for each hole (offsplice depths vs splice depths)

578 Table of species abbreviations for isotope tables

579 Leg 154 Combined benthic isotope data

580 Leg 154 Smoothed benthic isotope data

581 Site to site tie tables linking sites 925, 927, 928, and 929 to site 926

582 Core images (lighting corrected) for all Leg 154 cores in png format with depth scale and as depth scaled

583 Igor binary files